EPR and optical-absorption studies of Cu^{2+} in quasi-one-dimensional dichloro(1,2,4-triazole)Cu(II)

S. Subramanian
Département de Physique et G.R.S.D., Collège Militaire Royal de Saint-Jean, Saint-Jean-sur-Richelieu, Québec, Canada J0J 1R0

Sushil K. Misra and M. Bartkowski
Department of Physics, Concordia University, 1455 de Maisonneuve Boulevard West, Montreal, Quebec, Canada H3G 1M8

J. L. Thompson
Département de Chimie et G.R.S.D. Collège Militaire Royal de Saint-Jean, Saint-Jean-sur-Richelieu, Québec, Canada J0J 1R0
(Received 5 March 1984)

EPR measurements on dichloro(1,2,4-triazole)copper(II) have been made at room, liquid-nitrogen, and liquid-helium temperatures; in addition, its polarized absorption spectrum has been obtained at room temperature. The presence of the secondary EPR line below 57 K at approximately half the field at which the main line occurs, as well as the line shape of the main EPR line and the variation of its linewidth (at $\theta = 54.7°$ from the chain axis) as a function of temperature, confirms the quasi-one-dimensionality of the sample. From the angular variation of the linewidth the interchain interaction that is responsible for the departure from true one dimensionality was estimated to be $5.2 \times 10^{-3} J$, where J is the intrachain exchange constant. The g-tensor components for Cu^{2+} have been evaluated with use of a rigorous least-squares-fitting procedure. The temperature dependence of the linewidth shows good agreement with the theory of Cheung, Soos, Dietz, and Merritt [Phys. Rev. B 17, 1266 (1978)], proving the importance of spin diffusion in the long-time behavior of the spin correlation functions. Assignment of the polarized absorption spectrum has been made, and the data have been used to determine the degree of covalency in the metal-ligand bonding.

I. INTRODUCTION

An EPR investigation of the magnetic properties of dichloro(1,2,4-triazole)copper(II) (hereafter, DTC) was undertaken because of its interesting structural properties. X-ray analysis[1] of the complex shows that the neighboring nitrogen atoms of a triazole molecule coordinate to two copper atoms bridged by two chlorine atoms, the copper atoms being arranged in a one-dimensional array. A diagram of this chain is shown in Fig. 1. The Cu-Cu separation on a chain is 3.405 Å, while the minimum distance between two chains is 7.13 Å.[1] If the Cu^{2+} spins on a chain are coupled via exchange interaction, then the system should exhibit properties characteristic of a one-dimensional system, i.e., an isolated linear magnetic chain.[2,3] A fit of paramagnetic susceptibility data on this system yields a finite-length uniform Heisenberg antiferromagnetic chain with $J = 11$ K.[4,5] Recent works on linear-chain compounds[6,7] show that additional information concerning the interaction between localized spins can be obtained from EPR linewidth measurements.

It is the purpose of this paper to present detailed EPR data on DTC for various sample orientations and at temperatures from room down to liquid-helium temperature. The optical-absorption data on this sample have also been presented for completeness. For interpretation of the EPR linewidths the theory of Hughes, Morosin, Richards, and Duffy,[6] and that of Cheung, Soos, Dietz, and Merritt,[7] are used. The g-tensor components are computed using a rigorous least-squares-fitting procedure which simultaneously fits all of the EPR positions obtained for several orientations of the external magnetic field in three mutually perpendicular planes. Standard theory is used for the interpretation of optical-absorption data.

In Sec. II we deal with the crystal structure, sample preparation, and experimental details. The details of EPR spectra are given in Sec. III. The evaluation of g-tensor components is discussed in Sec. IV. In Sec. V we deal with the discussion of the presence of the "half-field" secondary EPR line as evidence of the quasi one dimensionality of the DTC. The interpretation of EPR linewidth variation of the main line is included in Sec. VI. The polarized optical spectrum and its interpretation is the subject of Sec. VII. The conclusions are summarized in Sec. VIII.

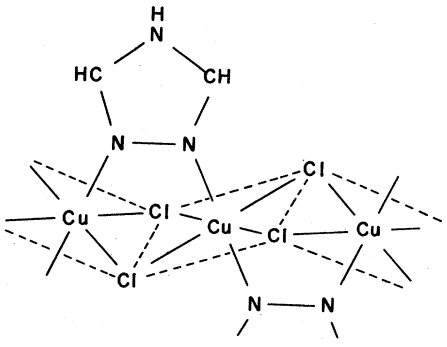

FIG. 1. Dichloro(1,2,4 - triazole)copper(II) structural unit; chain direction is along the crystallographic a axis.

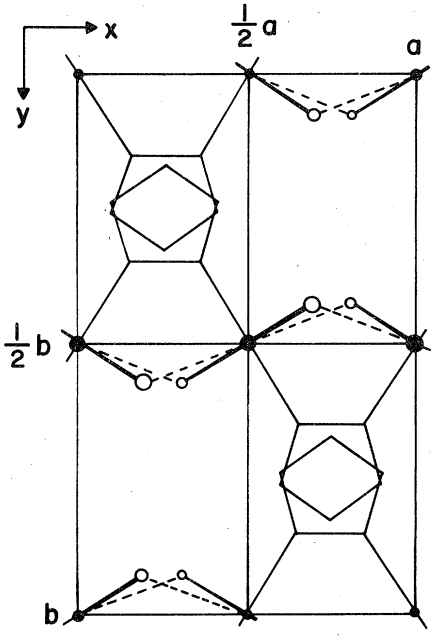

FIG. 2. c-axis projection of dichloro(1,2,4 - triazole) copper(II). ●, Cu atoms at $z=0$; ●, Cu atoms at $z=\frac{1}{2}$; ○, chlorine atoms. Pentagons represent triazole molecules.

II. CRYSTAL PREPARATION, STRUCTURE, AND EXPERIMENTAL DETAILS

Dark green single crystals were obtained by slow evaporation at room temperature of a 3-mol % HCl solution containing stoichiometric amounts of $CuCl_2$ and $C_2H_3N_3$. The x-ray data in the standard notation are monoclinic, space group $12/c$, $a=6.81$ Å, $b=11.93$ Å, $c=7.13$ Å, and $\beta=96°58'$. The crystal structure is exhibited in Fig. 2. There are two identical chains (magnetically equivalent in the ac plane) parallel to the a axis. Within the chain there are two slightly nonequivalent (magnetically) copper(II) sites per unit cell. This feature of the structure allows one to estimate the interchain interaction in the complex.

The X-band EPR measurements were carried out on a homodyne spectrometer equipped with 100-kHz field modulation at room, liquid-nitrogen, and liquid-helium temperatures. The b axis of the crystal was identified from precession photographs. The crystals were examined under a polarizing microscope; untwinned samples were selected for EPR measurements. The EPR measurements were performed for external-magnetic-field orientation in three mutually perpendicular planes defined by the three (mutually perpendicular) directions along which the EPR line positions exhibit extrema. (These directions will hereafter be referred to as z, x, and y, as arranged in increasing order of value.) The optical-absorption spectrum of the single crystal was measured at room temperature using a spectrophotometer equipped with polaroids.

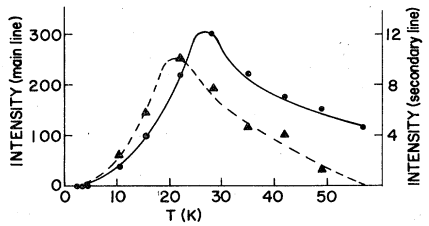

FIG. 3. Temperature variation of the intensities of the main (●) and half-field (△) lines in arbitrary units. The data points are connected by smooth lines.

III. EPR DATA

One strong, symmetric EPR line was observed down to nearly liquid-helium temperatures for all orientations of the crystal with respect to the magnetic field. This line disappeared below certain temperatures; the temperatures at which it disappeared being about 4.5, 5, and 7.5 K for $\vec{H}||\hat{z}$, $\vec{H}||\hat{x}$, and $\vec{H}||\hat{y}$, respectively.

In addition to this main line, a weak second line appeared below about 57 K at roughly half the main EPR line position. Its intensity (as measured in terms of its height) attained a maximum at about 20 K. Furthermore, it had the same intensity as that of the main line at about 5 K (see Sec. V for further discussion). The temperature and angular variations of the positions of these two lines near liquid-helium temperature are given in Figs. 3 and 4, respectively. The following discussion concentrates on the behavior of the main line only.

IV. ANALYSIS OF EPR DATA AND DISCUSSION

The EPR data were analyzed by simultaneously fitting all of the line positions obtained in the three mutually perpendicular planes using the method of least-square fitting,[8] minimizing χ^2, defined to be

$$\chi^2=\sum_i \left[\frac{|\Delta E_i|-h\nu_i}{\sigma_i}\right]^2, \tag{1}$$

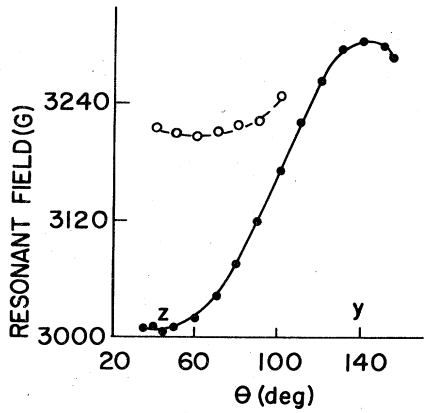

FIG. 4. Angular variation of the main (●) and half-field (○) lines in the z-y plane (liquid-helium temperature). The data points are connected by smooth lines.

TABLE I. Principal components of g tensor (square roots of principal values of g^2 tensor) at various temperatures.

Temperature	g_x	g_y	g_z
Room (300 kelvin)	2.0597±0.0005	2.0780±0.0005	2.2354±0.0004
Liquid nitrogen (77 kelvin)	2.0595±0.0004	2.0866±0.0005	2.2454±0.0004
Liquid helium (4.2 kelvin)	2.0364±0.0005	2.0942±0.0009	2.2419±0.0006

where ΔE_i is the calculated energy difference between the two levels ($M_S=\pm\frac{1}{2}$ of the Cu^{2+} ion, h is Planck's constant, ν_i is the Klystron frequency for the ith-line position, and σ_i is the weighting factor[9] for the ith-line position (it was assumed to be the uncertainty in locating the line center, roughly 10 G). For the simple case of $S=\frac{1}{2}$, one has[10]

$$(\Delta E_i)^2=\mu_B^2\vec{H}\cdot\vec{g}\cdot\vec{H}=\mu_B^2 g_{\text{eff}}^2 H^2 , \tag{2}$$

where

$$g_{\text{eff}}^2=(g^2)_{zz}n^2+2(g^2)_{zx}nl+(g^2)_{xx}l^2 +2(g^2)_{zy}nm+(g^2)_{yy}m^2+2(g^2)_{xy}lm , \tag{3}$$

with l,m,n denoting the direction cosines of $\vec{H}$ with respect to the crystalline axes x,y,z and $(g^2)_{\alpha\beta}$; $\alpha,\beta=x,y,z$ denote the components of the g^2 tensor. Since $(g^2)_{\alpha\beta}=(g^2)_{\beta\alpha}$, there are only six independent components of the g^2 tensor. Using (2) it is easy to calculate the derivatives of χ^2 required for the least-squares-fitting procedure.[8]

The components of the g^2 tensor so determined from the data obtained at the three temperatures were diagonalized and the principal g values (square root of the principal components of the g^2 tensor) along with their associated uncertainties[9] are listed in Table I. The elements of the unitary matrix which diagonalized the g^2 tensor at room temperature are given in Table II. If one knows the relationship of the z, x, and y magnetic axes to the crystallographic axes, one can determine, using this unitary matrix, the relative orientations of the crystallographic and the principal g axes. In the present case, the x, y, z, and principal g axes almost coincide.

V. SECONDARY HALF-FIELD EPR LINE (SIDEBAND)

It has been experimentally found that, for low- (one- or two-) dimensional paramagnetic solids, a sideband on main EPR line appears at half its Zeeman field [e.g., $(CH_3)_4NMnCl_3$ (TMMC); $CuCl_2\cdot 2NC_5H_5$ (CPC); copper benzoate; K_2MnF_4].[11–13] The theory[14] shows that in such systems the main EPR line is determined by the total dipolar correlation function, $\psi(\tau)$. Furthermore, it has been shown[14] that if $\psi(\tau)$ is expressed as $\sum_M \psi_M(\tau)\exp(iM\omega_0\tau)$ (where M is the total change in Zeeman quantum number and $\omega_0/2\pi$ is the resonance frequency), then the half-field line comes from the real part of the nonsecular term in $\psi(\tau)$ corresponding to $M=1$, i.e., $\psi_1(\tau)\cos(\omega_0\tau)$. The observation of this sideband provides a direct confirmation of the effect of long-time persistence of spin correlation functions for low-dimensional systems.[15–18] The theory of the anisotropy of intensity and linewidth has been given by Komatsubara and Nagata,[19] as well as by Nagata and Okuda.[13]

As seen from Fig. 3 there is unequivocal evidence of the presence of this sideband at half-field in DTC, confirming the low dimensionality of this system. [Since the present measurements do not give sufficiently detailed variation of the linewidth (angular or temperature) of this sideband, no further analysis of this line would be carried out here.]

TABLE II. Direction cosines of the principal axes of the g^2 tensor with respect to the magnetic (x,y,z) axes at room temperature. [Elements of the matrix that diagonalizes the g^2 tensor as expressed in the (x,y,z) system.]

0.0046	−0.0444	0.9990
−0.0142	−0.9989	−0.0443
0.9999	−0.0139	−0.0052

VI. LINEWIDTH BEHAVIOR OF THE MAIN LINE

There are two identical chains (magnetically equivalent in the a-c plane) in DTC parallel to the crystallographic a axis. (Hereafter, in conformity with standard notation, the chain axis will be referred to as the c axis.) Within the chains there are two slightly magnetically inequivalent Cu^{2+} ions per unit cell. The direction of the tetrogonal axis of these two ions is shown in Fig. 5. If the interchain exchange interaction J' were sufficiently small, one would, in general, observe two distinct (main) EPR lines.

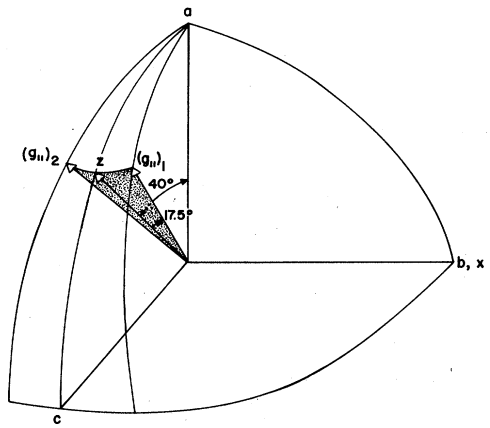

FIG. 5. Definitions of the crystallographic (a,b,c) and magnetic axes (x,y,z) in DTC. $(g_{\|})_1$ and $(g_{\|})_2$ are the g components parallel to the tetragonal axes of sites 1 and 2, respectively.

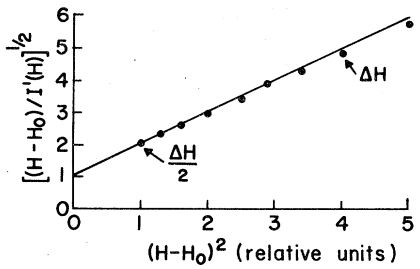

FIG. 6. Ordinates and absissas in this figure as calculated from the EPR derivative spectrum are such that they yield a straight line for a Lorentzian line shape. The data (●) and theory (solid line) are normalized to a slope of 1 and a value of 1 at the origin (Ref. 3).

However, in practice, J' averages these two lines, so only one composite main EPR line is observed at all temperatures of observation in the case of DTC. (This is also found to be true in other Cu complexes, e.g., $CuCl_2 \cdot 2NC_5H_5$.[6])

A. Determination of the dimensionality of DTC

In order to decide whether DTC is one- or two-dimensional system the following consideration was used. If the system is indeed two dimensional, the linewidth should be the same for all orientations of the external field in one of the planes x-y, y-z, or z-x, where x,y,z are the magnetic axes. Since this is not the case for DTC, it is ruled out that DTC is a two-dimensional system.

It is well known[2] that the line shape of truly one-dimensional compounds is given by the Fourier transform of $\exp(-At^{3/2})$, intermediate between Gaussian and Lorentzian, for all orientations of the external field, except at $\theta=54.7°$ (i.e., when $3\cos^2\theta-1=0$, the angle θ being measured from the chain axis), at which angle the line shape is Lorentzian (for an excellent discussion of line shapes, see Kokozka[20]). However, even slight departure from true one dimensionality renders the line shape Lorentzian for all orientations of the magnetic field.[6] This is what is observed in the present case; see Fig. 6 for $\theta=0°$. That DTC is a quasi-one-dimensional system is confirmed by the fact that the fitting of the EPR linewidth (at $\theta=54.7°$ from the chain axis) as a function of temperature, using the diffusive assumption of Cheung *et al.*,[7] is excellent, as exhibited by Fig. 7. The part of their theory that is relevant to the interpretation of the present experimental results is given below.

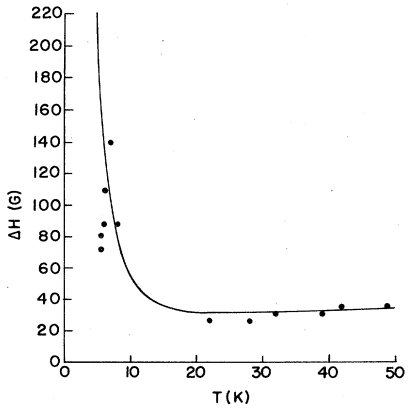

FIG. 7. Temperature dependence of the EPR absorption of DTC at X band. The full width at half-height ΔH as determined from the derivative line shape ($\Delta H=\sqrt{3}\,\Delta H_{pp}$) is shown for the magnetic field parallel to the z axis ($\theta=54.7°$). The solid line is based on Eq. (B6), as discussed in Appendix B.

B. Temperature variation of the linewidth

Theoretical. The EPR line shape is given by

$$I(\Omega)=\frac{1}{2\pi}\int_{-\infty}^{+\infty}\phi(t)\exp(-i\Omega t)dt\ , \tag{4}$$

where $I(\Omega)$ is the intensity at frequency Ω, and the time evolution of the relaxation function $\phi(t)$ satisfies

$$\phi(t)=-\int_0^t dt\,\psi(t-\tau)d\tau\ . \tag{5}$$

In Eq. (5) the total spin torque correlation function $\psi(t)$ is assumed to be

$$\psi(t)=\psi_{KT}(t)\exp(-a\Omega_{1/2}t)\ , \tag{6}$$

where a is an adjustable parameter satisfying $a\gtrsim 1$, and $\Omega_{1/2}$ is the observed half-width. $\psi_{KT}(t)$ is the correlation function in the Kubo-Tomita approximation. For a one-dimensional system, $\Psi_{KT}(t)$ contains short-time and diffusive contributions,

$$\psi_{KT}(t)=\psi_s(t)+\psi_d(t)\ . \tag{7}$$

$\psi_s(t)$ contributes solely to the Lorentzian line shape, while only the nonsecular parts ($M=1,2$) of $\psi_d(t)$ contribute to the Lorentzian line shape. The corresponding expressions for the Lorentzian half-widths $\Delta\omega_{1/2}$ and Γ_M for short-time and diffusive contributions, respectively, are given in Appendix A. The $M=0$ part of $\psi_d(t)$, however, gives a non-Lorentzian contribution to the linewidth, as discussed by Cheung *et al.*[7] This cannot be explicitly estimated. However, the overall half-width including the Lorentzian contributions as discussed in Appendix A, and the non-Lorentzian contribution due to $\psi_d(t)$ for $M=0$, can be obtained by solving an algebraic equation for the reduced half-width x [$\equiv(\Omega_{1/2}/\Gamma)^{1/2}$]. This is given in Appendix B.

From Appendixes A and B it is clear that Γ and B [Eqs. (A17) and (B2), respectively] depend on the temperature via the intermediary of the diffusion coefficient $D(T)$, thereby making the temperature dependence of the linewidth a factor.

Experimental. The data for the full width ΔH at $\theta=54.7°$ is shown in Fig. 7. It may be seen that the linewidth attains a sharp maximum around 7 K, below which the line disappears rapidly. The solid curve is based on Eq. (B6), calculated with the value of the cutoff parameter $a=1.5$. The agreement with theory[7] is seen to be quite good. It should be noted that the theory of Cheung *et al.* is applicable only for the temperature range at which the exchange Hamiltonian is isotropic. It will thus break down at temperatures where thermal averages

over Zeeman and dipolar Hamiltonians produce anisotropies.[7]

The adjustable parameter a cannot be rigorously estimated as its value depends upon compromises among accurate determination of spin correlation functions in $\psi_{KT}(t)$ and various decoupling schemes. However, it may be shown to be related to the secular (long-time) cutoff time t_0 ($\sim\tau_2$ in Fig. 1 of Ref. 7) by

$$a\Omega_{1/2}\sim t_0^{-1} .$$

C. Angular variation of linewidth at room temperature

The second moment (M_2) of the resonance line in the case of three-dimensional interactions has been calculated by Van Vleck.[21] If the exchange interaction is less than the Zeeman interaction, only the secular part of the dipolar interaction contributes to the linewidth, and M_2 is given by

$$M_2=\tfrac{3}{4}\gamma_e^4\hbar^2S(S+1)\sum_j{}'r_{ij}^{-6}(3\cos^2\theta_{ij}-1)^2 . \quad (8)$$

The sum is over j only and the prime over the summation sign indicates that $j\neq i$. $\vec{r}_{ij}$ is the vector connecting the spins i and j, and it makes an angle θ_{ij} with the magnetic field. In the opposite case (exchange interaction greater than Zeeman interaction), both secular and nonsecular terms of the dipolar interaction contribute and the second moment is given by[20]

$$M_2=\tfrac{3}{2}\gamma_e^4\hbar^2S(S+1)\sum_j{}'r_{ij}^{-6}(1+\cos^2\theta_{ij}) . \quad (9)$$

The angular variation of the linewidth at room temperature in the a-c plane is shown in Fig. 8. It is clear that Eq. (9) cannot at all explain this result, because it does not predict the experimentally observed linewidth minimum at $\theta=54.7°$. On the other hand, Eq. (8) does predict this minimum and so in this paper the second moment has been calculated only according to Eq. (8), and drawn in Fig. 8 as the dashed line. [For comparison, the second moment along $\theta=97°$ was set equal to the observed linewidth for the magnetic field parallel to the a axis. It may be seen, however, that the experimental values depart significantly from those calculated according to Eq. (8).] However, the linewidth calculated according to the theory of Cheung *et al.* (solid line in Fig. 8) clearly shows good qualitative agreement with the experimental data. (The value of $a=1.5$ has been used for calculating the linewidth; this gives the best agreement for the temperature variation of the linewidth.) The observed angular variation of the linewidth is thus far more in agreement with the theory of Cheung *et al.* than that of Van Vleck [Eq. (8)].

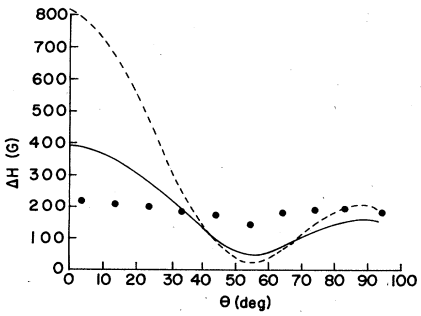

FIG. 8. Angular dependence of the full width at half-height ΔH as determined from the derivative line shape ($\Delta H=\sqrt{3}\,\Delta H_{pp}$) of DTC at 300 K in the a-c plane. The solid curve is based on Eq. (B6), while the dashed line is the second moment calculated according to Eq. (8) (see Sec. VI).

D. Interchain exchange (J')

As mentioned earlier, DTC contains two magnetically equivalent chains. Within the chains there are two magnetically inequivalent Cu^{2+} sites. If the interchain exchange interaction J' is sufficiently small, then one would see two EPR lines for many orientations of the external magnetic field; the difference in the corresponding resonant field positions would be proportional to the microwave frequency.[22] J' tends to average these two lines, and in the case of DTC, J' is sufficiently large so that only one line is observed. A rough determination of J'/J (where J is the intrachain exchange) can be made using the frequency dependence of the linewidth due to anisotropic dipolar interactions between adjacent chains to determine the Fourier components of the spin correlation function.[23] This method will not be used here because the present measurements were carried out only at one frequency. The theory of Hughes, Morosin, Richards, and Duffy[6] will instead be used to determine J'. The frequency-dependent peak-to-peak linewidth lw, in gauss, due to the exchange-coupled adjacent sites, is

$$lw=(\delta H)^2/H_e . \quad (10)$$

Here, δH is the splitting which would be observed had the coupling between chains been zero (thus the EPR lines due to the two sites are resolved) and H_e is an effective field which expresses the actual coupling. According to theory,[22] this splitting in the absence of interchain coupling has its maximum in the plane containing the b axis and the $g_{\|}$ axes of the two sites (in the present case, the z-x plane). To lowest order in $(g_{\|}-g_{\perp})/(g_{\|}+g_{\perp})$, of any one site at 9.42 GHz,

$$\delta H=160\,\sin(2\omega) , \quad (11)$$

where ω is the angle between the field and the b axis in the z-x plane, and $g_{\|}$ and $g_{\perp}$ refer to the g values of the individual sites. Least-squares-fitting of the angular variation of g in the z-x and z-y planes gave $g_{\|}=2.253$ and $g_{\perp}=2.060$. The observed linewidth in the z-x plane was least-squares-fitted to Eq. (10); it gave a value of $H_e=1500$ G as the best fit for the exchange field. In the case of DTC, the exchange field H_e is related to J' by[6]

$$\gamma_eH_e=\frac{21.65}{\hbar}\frac{|J'|^{4/3}}{|J|^{1/3}} . \quad (12)$$

J', as calculated using Eq. (12), is

$$J'=5.2\times10^{-3}J .$$

This result is consistent with the theoretical prediction of Hennessey, McElwee, and Richards[24] which states that if the line shape is found to be Lorentzian at all angles to the chain, J'/J should be greater than 10^{-3}. (The value reported for CPC is 12×10^{-3}.[6])

VII. POLARIZED OPTICAL-ABSORPTION SPECTRUM

The optical-absorption spectrum of the single crystal of DTC reveals the presence of three bands, at 16.3, 15.0, and 10.2 kK (1 kK$\equiv10^3$ kayser $=1000$ cm^{-1}), the band at 15.0 kK being the only one that is strongly polarized. For a proper identification of these bands, the ground state should be known. The ^{2}D state of the free Cu^{2+} ion is split into four levels of symmetry, B_{1g}, A_{1g}, B_{2g}, and E_g, by the crystal field of D_{4h} point-group symmetry;[25] while the first three are singlets, the last is a doublet. The fact that $g_{\|}>g_{\perp}$ uniquely establishes that the ground state is B_{1g}, corresponding to a hole in the $d_{x^2-y^2}$ orbitals (the parallel and perpendicular directions are defined with respect to the tetragonal axis). The values of the (purely electric) dipole integrals responsible for the various transitions to the ground state are given in Table III. All of these transitions are orbitally forbidden, but become vibronically allowed, except for the $B_{2g}\rightarrow B_{1g}$ transition in the z polarization, through the perturbing vibrations A_{2u}, B_{2u}, and E_u.[26] The band at 15.0 kK is thus assigned to the $d_{xy}\rightarrow d_{x^2-y^2}$ transition because of its polarization. There is some ambiguity regarding the other two transitions, but it is likely that the more intense band at 16.3 kK is due to the transition to the (excited) $E_g(d_{xy,yz})$ state on account of its double degeneracy.

The usual expressions[27] for $g_{\|}$ and $g_{\perp}$ in an axial field, taking into account the reduction in spin-orbit–coupling constant, as well as the orbital reduction, are

$$g_{\|}=2[1-4k_{\|}^2(\lambda/\Delta_2)]$$

and (13)

$$g_{\perp}=2[1-k_{\perp}^2(\lambda/\Delta_3)]\ ,$$

where Δ_2 and Δ_3 are the energies of the $B_{2g}\rightarrow B_{1g}$ and $E_g\rightarrow B_{1g}$ transitions for the D_{4h} point group, λ is the spin-orbit–coupling constant, and the empirical parameter k includes both the above reductions. With the use of the values $\Delta_2=15.0$ kK, $\Delta_3=16.3$ kK, $\lambda=-0.829$ kK, $g_{\|}=2.253$, and $g_{\perp}=2.060$, the values $k_{\|}=0.76$ and $k_{\perp}=0.78$ are deduced. Since these values are clearly less than unity, they indicate[28] that the metal-ligand bonding are considerably covalent for the Cu^{2+} ion. However, in the absence of hyperfine-structure data, it is not possible to describe the complete nature of the bonding.[29]

VIII. CONCLUDING REMARKS

The most important conclusion of the present work is that DTC is a quasi-one-dimensional system whose EPR linewidth is determined by the long-term persistence of the spin correlation functions as revealed by (i) the presence of the secondary half-field EPR line, (ii) the Lorentzian nature of the line shape of the main EPR line for all orientations of the external magnetic field, (iii) the behavior of the angular and temperature variation of the linewidth, and (iv) the particular (nonzero) value of the interchain exchange constant J' (i.e., of the order of $10^{-3}J$, where J is the intrachain exchange constant).

It would be of interest to study the angular and temperature variation of the secondary line in detail; several such studies have recently been published for other samples.[13,19] The data of the present work do not contain sufficient details on this aspect; however, a detailed experimental study of this problem is currently in progress by us.

ACKNOWLEDGMENTS

We are grateful to the Natural Sciences and Engineering Research Council of Canada for financial support (Grant No. A4485). The use of the facilities provided by the Concordia University Computer Centre is gratefully acknowledged. One of us (S.S.) is grateful to Dr. C. Y. Cheung and Dr. A. H. Reddoch for their interest in this problem.

APPENDIX A: CONTRIBUTIONS TO THE LORENTZIAN LINEWIDTH

The short-time contribution $\psi_s(t)$ leads to a Lorentzian line with half-width[7]

$$\Delta\omega_{1/2}=(\pi/2)^{1/2}(M_2/\omega_e)\ , \tag{A1}$$

where

$$M_2=\frac{3\zeta(6)}{c^6}\gamma_e^4\hbar^2S(S+1)(1+\cos^2\theta)f(K) \tag{A2}$$

and

$$\omega_e^2=\tfrac{192}{15}S(S+1)\frac{J^2}{\hbar^2}\frac{g(K)}{f(K)}\ . \tag{A3}$$

In Eqs. (A2) and (A3),

TABLE III. Representations of the integrands of the various electric dipole integrals for the D-state ion in D_{4h} symmetry, according to their transformation properties. B_{1g} is the ground state, while A_{1g}, B_{2g}, and E_g are excited states. ψ_e and ψ_e' are the wave functions corresponding to the ground and excited states.

Integrand	$A_{1g}\rightarrow B_{1g}$	$B_{2g}\rightarrow B_{1g}$	$E_g\rightarrow B_{1g}$
$\psi_e' z\psi_e$	B_{2u}	A_{1u}	E_u
$\psi_e'(x,y)\psi_e$	E_u	E_u	$A_{1u}+A_{2u}+B_{1u}+B_{2u}$

$$\zeta(6)=\sum_n n^{-6}=1.06\ , \tag{A4}$$

$$\gamma_e=g\mu_B/\hbar\ , \tag{A5}$$

$$f(K)=\frac{1-u}{1+u}\left[1+\frac{v}{5}+\frac{12u^2}{5(1-v)}\right]\ , \tag{A6}$$

$$g(K)=\frac{1-u}{1+u}\left[\frac{9vK}{8}(1-u)^2-3uK\left[1-\frac{3u+v}{4}\right]\right]\ , \tag{A7}$$

$$K=kT/2|J|S(S+1)\ . \tag{A8}$$

In Eqs. (A6) and (A7),

$$u=K-\coth(1/K)\ , \tag{A9}$$

$$v=1+3uK\ . \tag{A10}$$

In Eq. (A2), $c=3.405$ Å is the distance between adjacent spins along the chain axis and $|J|=15.2\times10^{-16}$ erg is the antiferromagnetic exchange.

The nonsecular parts ($M=1,2$) of the diffusive contribution $\psi_d(t)$ lead to the Lorentzian half-width

$$\Gamma_M=\frac{\zeta^2(3)S(S+1)F_M^2(\theta)N(K)}{3\{M[D(T)\omega_0/c^2]\}^{1/2}}\left[1-2\left[\frac{4M\omega_0}{\pi\omega_e}\right]^{1/2}\right]\ , \quad M=1,2 \tag{A11}$$

where

$$F_1(\theta)=(90)^{1/2}\frac{\gamma_e^2\hbar\sin\theta\cos\theta}{2c^3}\ , \tag{A12}$$

$$F_2(\theta)=\frac{3\gamma_e^2\hbar\sin\theta}{2c^2}\ , \tag{A13}$$

and

$$N(K)=\frac{6}{5(1-v)}+\frac{5+v}{5(1-u^2)}\ . \tag{A14}$$

Here, $\zeta^2(3)=\sum_n n^{-3}=1.20$ and D is the diffusion constant proportional to J and depending on T. For classical spins, one has

$$\frac{D(T)}{D(\infty)}=\frac{1-u}{1+u}\ , \tag{A15}$$

where

$$D(\infty)=2.78[S(S+1)]^{1/2}|J|c^2/\hbar\ . \tag{A16}$$

Both the short-time contributions and the nonsecular diffusive terms thus lead to a half-width

$$\Gamma=\Delta\omega_{1/2}+\Gamma_1+\Gamma_2\ . \tag{A17}$$

APPENDIX B: OVERALL HALF-WIDTH

The secular component ($M=0$) of the diffusive term is given by

$$\psi_{d0}(t)=B(\pi t)^{-1/2}\ , \tag{B1}$$

where

$$B=\frac{2\zeta^2(3)N(K)S(S+1)}{3[2D(T)/c^2]^{1/2}}F_0^2(\theta)\ . \tag{B2}$$

In Eq. (B2),

$$F_0(\theta)=\frac{3\gamma_e^2\hbar(3\cos^2\theta-1)}{2c^3}\ . \tag{B3}$$

Substitution of Eqs. (5) and (6) into Eq. (4) leads to an algebraic equation for the reduced overall half-width $x=(\Omega_{1/2}/\Gamma)^{1/2}$,

$$x^6-2x^3P(a)\beta\sin\delta-x^2-2x\beta a^{-1/2}-\beta^2P(a)[2a^{-1/2}\cos\delta-P(a)]=0\ , \tag{B4}$$

where $\beta=B/\Gamma^{3/2}$ and $P(a)=(1+a^2)^{-1/4}$. The angle δ satisfies

$$\cos(2\delta)=\gamma/(\Omega^2+\gamma^2)^{1/2}\ , \tag{B5}$$

with $\gamma=a\Omega_{1/2}$. There is only one positive root of Eq. (B4) which yields $\Omega_{1/2}$. The full width in gauss is then

$$\Delta H=2\Omega_{1/2}/\gamma_e\ . \tag{B6}$$

The cutoff parameter a and the temperature dependence of ΔH are determined from the theoretical fit of the experimental data and from the coefficients Γ and B in Eqs. (A17) and (B2), respectively.

[1] J. A. Jarvis, Acta Crystallogr. **15**, 964 (1962).
[2] R. E. Dietz, F. R. Merritt, R. Dingle, D. Hone, B. G. Silbernagel, and P. M. Richards, Phys. Rev. Lett. **26**, 1186 (1971).
[3] R. R. Bartkowski and G. Morosin, Phys. Rev. B **6**, 4209 (1972).
[4] M. Inoue, S. Emori, and M. Kubo, Inorg. Chem. **7**, 1427 (1968).
[5] Y. Lepine, V. Larochelle, A. Caillé, and J. L. Thompson, Phys. Status Solidi B **91**, K111 (1979).
[6] R. C. Hughes, B. Morosin, P. M. Richards, and W. Duffy, Jr., Phys. Rev. B **11**, 1795 (1975); for a review, see P. M. Richards, in *Low-Dimensional Cooperative Phenomena*, edited by H. J. Keller (Plenum, New York, 1975), p. 147.
[7] T. T. P. Cheung, Z. G. Soos, R. E. Dietz, and F. R. Merritt, Phys. Rev. B **17**, 1266 (1978).
[8] S. K. Misra, J. Magn. Reson. **23**, 403 (1976).
[9] S. K. Misra and S. Subramanian, J. Phys. C **15**, 7199 (1982).
[10] J. E. Wertz and J. R. Bolton, *Electron Spin Resonance* (McGraw-Hill, New York, 1972), p. 136.
[11] P. M. Richards and M. B. Salamon, Phys. Rev. B **9**, 32 (1974).
[12] Y. Ajiro, S. Matsukawa, T. Yamada, and T. Haseda, J. Phys. Soc. Jpn. **39**, 259 (1975).
[13] K. Nagata and K. Okuda, J. Phys. Soc. Jpn. **46**, 1726 (1979).
[14] G. E. Pake, *Paramagnetic Resonance* (Benjamin, New York, 1962), p. 135.
[15] A. Lagendijk and D. Schoemaker, Phys. Rev. B **16**, 47 (1977).
[16] K. Nagata, I. Yamada, T. Komatsubara, and T. Nishizaki, J. Phys. Soc. Jpn. **43**, 707 (1977).
[17] M. Hamashima and Y. Ajiro, J. Phys. Soc. Jpn. **44**, 1743

(1978).
[18]Y. Yokozawa and M. Tanimoto, J. Phys. Soc. Jpn. **44**, 1741 (1978).
[19]T. Komatsubara and K. Nagata, J. Phys. Soc. Jpn. **45**, 826 (1978).
[20]G. F. Kokozka in *Low Dimensional Cooperative Phenomena,* Ref. 6, p. 171.
[21]J. H. Van Vleck, Phys. Rev. **74**, 1168 (1948).
[22]B. R. McGarvey, in *Transition Metal Chemistry,* edited by R. Carlin (Dekker, New York, 1966) Vol. 3, p. 89.
[23]Z. G. Soos, T. Z. Huang, J. S. Valentine, and R. C. Hughes, Phys. Rev. B **8**, 993 (1973); T. Z. Huang and Z. G. Soos, *ibid.* **9**, 4981 (1974).
[24]M. J. Hennessy, C. D. McElwee, and P. M. Richards, Phys. Rev. B **7**, 930 (1973).
[25]D. W. Smith, Inorg. Chem. **5**, 2236 (1966).
[26]D. C. Harris and M. D. Bertolucci, *Symmetry and Spectroscopy* (Oxford University Press, New York, 1978), p. 338.
[27]C. J. Ballhausen, *Introduction to Ligand Field Theory* (McGraw-Hill, New York, 1962) pp. 134 and 268.
[28]D. E. Billing and B. J. Hathaway, J. Chem. Soc. **A** 1516 (1968).
[29]A. H. Maki and B. R. McGarvey, J. Chem. Phys. **29**, 31 (1958).